Neurobiology of Aging 69 (2018) 68–75

Contents lists available at ScienceDirect

Neurobiology of Aging

journal homepage: www.elsevier.com/locate/neuaging

Telomere attrition is associated with declines in medial temporal lobe volume and white matter microstructure in functionally independent older adults

Adam M. Staffaroni [a,*], Duygu Tosun [b,c], Jue Lin [d], Fanny M. Elahi [a], Kaitlin B. Casaletto [a], Matthew J. Wynn [a], Nihar Patel [a], John Neuhaus [e], Samantha M. Walters [a], Elissa S. Epel [f], Elizabeth H. Blackburn [g], Joel H. Kramer [a]

[a] Department of Neurology, Memory and Aging Center, University of California at San Francisco, San Francisco, CA, USA
[b] Department of Veteran Affairs Medical Center, San Francisco, CA, USA
[c] Department of Radiology and Biomedical Imaging, University of California at San Francisco, San Francisco, CA, USA
[d] Department of Biochemistry and Biophysics, University of California at San Francisco, San Francisco, CA, USA
[e] Department of Epidemiology and Biostatistics, University of California, San Francisco, USA
[f] Department of Psychiatry, University of California at San Francisco, San Francisco, CA, USA
[g] Salk Institute for Biological Sciences, La Jolla, CA, USA

ARTICLE INFO

Article history:
Received 7 January 2018
Received in revised form 29 March 2018
Accepted 28 April 2018
Available online 8 May 2018

Keywords:
Aging
Biomarker
Memory
Hippocampus
Longitudinal
Diffusion tensor imaging (DTI)
Fornix
MRI
Neuroimaging

ABSTRACT

Although leukocyte telomere length (TL) shortens over the lifespan and is associated with diseases of aging, little is known about the relationships between TL, memory, and brain structure. Sixty-nine functionally normal older adults (mean age = 71.7) were assessed at 2 time points (mean interval = 2.9 years). Linear mixed models assessed relationships between TL and hippocampal volume, fractional anisotropy, and mean diffusivity (MD) of the fornix and verbal and visual episodic memory. Unstandardized coefficients are reported in the following, and p values are not corrected for multiple comparisons. A negative baseline trend was observed between TL and fornix MD ($b = -0.01$, $p = 0.06$), but no other cross-sectional associations were significant ($ps > 0.16$). Greater TL shortening at follow-up was associated with greater hippocampal volume loss ($b = 27.09$, $p < 0.001$), even after controlling for global volume loss ($b = 10.83$, $p = 0.002$). Greater telomere attrition was also associated with larger increases in fornix MD ($b = -0.01$, $p = 0.012$) and decreases in fornix fractional anisotropy ($b = 0.004$, $p = 0.002$). TL was not associated with changes in episodic memory ($ps > 0.23$). These relationships may reflect neurobiological influences that affect both TL and brain structure, as well as the effect of TL on brain aging via mechanisms such as cellular senescence and inflammation.

1. Introduction

Telomeres are a complex of short DNA repeats and protective proteins positioned at the end of chromosomes (Sfeir and de Lange, 2012). They serve the critical role of protecting genomic DNA by preventing degradation (Blackburn et al., 2006). The DNA replication mechanism prevents the complete copying of telomeric DNA, resulting in progressive shortening of telomeres across the lifespan. This process is highly regulated, however, and the rate of telomere attrition is variable within and across individuals. Telomere length (TL) is a reflection of a lifetime of systemic influences on cellular health; for example, TL is affected by damaging processes such as DNA replication stress, oxidative damage, and inflammation, and TL is related to many risk factors for common diseases of aging (Blackburn et al., 2015). TL is not only a consequence of the neurobiology of aging, but telomere shortening can in turn promote cellular senescence (Sahin et al., 2011), inflammation (Ghosh et al., 2012), and accelerated aging (Armanios and Blackburn, 2012).

Despite the clear connection between TL and aging biology, relatively little is known about TL and markers of brain health in older adults, including its usefulness as a monitoring tool. The episodic memory system is one of the first brain networks affected in pathological aging processes such as Alzheimer's disease (AD) and hippocampal sclerosis. The hippocampus is the seat of episodic memory and is connected to other areas important for memory, collectively

* Corresponding author at: Postdoctoral Fellow, Department of Neurology, Memory and Aging Center, University of California, San Francisco, San Francisco, CA 94158. Tel.: +1 415 502 7201; fax: +1 415 476 2921.
E-mail address: Adam.Staffaroni@ucsf.edu (A.M. Staffaroni).

0197-4580/$ – see front matter © 2018 Elsevier Inc. All rights reserved.
https://doi.org/10.1016/j.neurobiolaging.2018.04.021

referred to as the Papez circuit, via a white matter tract known as the fornix (Oishi and Lyketsos, 2014). Abnormal decline in the structure of the hippocampus and fornix, quantified using neuroimaging, is a harbinger for pathological aging. Volume loss in the hippocampus predicts poorer cognitive trajectories in older adults (Dumurgier et al., 2017; Fletcher et al., 2018), and diffusion tensor imaging (DTI) quantification of fornix microstructure is a sensitive early predictor of cognitive decline in cognitively normal older adults (Fletcher et al., 2013) and predicts cognitive decline and progression to AD in patients with mild cognitive impairment (MCI) (Mielke et al., 2012).

Although TL is associated with hippocampal volume in cross-sectional analyses (Grodstein et al., 2008; Jacobs et al., 2014; King et al., 2014), no longitudinal studies have systematically examined the relationship between TL, memory and its neural correlates, including the role of white matter microstructure. Deeper characterization of this relationship in otherwise clinically normal older adults may support the role of TL as a preclinical marker of early pathological brain changes. We therefore aimed to determine the degree to which baseline TL and the rate of telomere attrition were associated with verbal and visual episodic memory, hippocampal volumes, and DTI quantification of the fornix in typically aging adults.

2. Materials and methods

2.1. Participants

Participants were community-dwelling older adults recruited at the University of California, San Francisco (UCSF), Memory and Aging Center as part of a larger longitudinal study that recruits adults over age 50. The sample included neurologically and functionally intact older adults who received baseline and follow-up structural and diffusion weighted imaging scans, cognitive testing, and a blood draw for DNA as part of a comprehensive evaluation. All subjects were reviewed at a case conference with a board-certified neuropsychologist and neurologist. The neurologic and neuropsychological examination was used to determine that participants were neurologically normal. Informant interview (Clinical Dementia Rating Scale [CDR]) was also used; all participants had a CDR = 0 at baseline, indicating that there were no functional impairments. Baseline exclusion criteria included syndromic diagnosis of dementia or MCI according to consensus research criteria (Albert et al., 2011; McKhann et al., 2011), neurological conditions that may affect cognition (e.g., epilepsy, stroke, Parkinson's disease), significant systemic medical illnesses, severe psychiatric illness (e.g., bipolar disorder, schizophrenia), a substance use diagnosis within 20 years, or current moderate to severe depression (Geriatric Depression Scale $\geq$15 of 30). Two participants showed mild cognitive changes at follow-up (CDR = 0.5). The final data set included 69 participants. Demographic data are provided in Table 1. All participants provided written informed consent, and the UCSF Committee on Human Research approved the study protocol.

2.2. Telomere quantification methods

Genomic DNA was isolated from whole blood using an automated purification system (Autopure LS; Qiagen). The leukocyte TL measurement assay was adapted from the original published method by Cawthon (Cawthon, 2002; Lin et al., 2010). The telomere thermal cycling profile consists of: cycling for T (telomic) polymerase chain reaction (PCR): 96 °C for 1 minute, denature at 96 °C for 1 second, anneal/extend at 54 °C for 60 seconds, with fluorescence data collection, 30 cycles.

Cycling for S (single-copy gene) PCR: 96 °C for 1 minute; denature at 95 °C for 15 seconds, anneal at 58 °C for 1 second, extend at 72 °C for 20 seconds, 8 cycles; followed by denature at 96 °C for 1 second, anneal at 58 °C for 1 second, extend at 72 °C for 20 seconds, hold at 83 °C for 5 seconds with data collection, 35 cycles.

Table 1
Demographics

Measure/characteristic	Mean (SD or IQR)
Baseline telomere length (T/S ratio)	1.1 (0.2)
Years between baseline and follow-up	2.9 (0.6)
Demographics	
Age	71.7 (6.8)
Education	17.7 (2.3)
Female (%)	58.0
Baseline cognition	
MMSE	30 (29.30)
CVLT-II LDFR	12.3/16 (2.8)
Benson figure recall	11.25/17 (2.2)
Health history, n (%)	
APOE ε4 carriers	24 (34.8)
Presence of vascular factors	
Current smoker	4 (5.8)
Remote heart attack	1 (1.4)
History of hypertension	23 (33.3)
History of hypercholesterolemia	37 (53.6)
History of diabetes	1 (1.4)
Vascular risk score: mean (SD)	1 (0.7)
PASE score: mean (SD)	132.0 (61.7)
Baseline neuroimaging (mm^3)	
Gray matter volume	607,300.7 (54,184.3)
Hippocampal volume	5252.2 (485.7)
Fornix FA	0.41 (0.03)
Fornix MD	0.71 (0.1)

T/S ratio compares telomere length to a reference sample.
Key: CVLT-II LDFR, California verbal learning test second edition long delay-free recall; FA, fractional anisotropy; IQR, interquartile range; MD, mean diffusivity; mm^3, cubic millimeters; MMSE, mini mental state examination; PASE, the physical activity scale for the elderly.

The primers for the telomere PCR were *tel1b* [5′-CGGT TT(GTTTGG)$_5$GTT-3'], used at a final concentration of 100 nM, and *tel2b* [5′-GGCTTG(CCTTAC)$_5$CCT-3'], used at a final concentration of 900 nM. The primers for the single-copy gene (human beta-globin) PCR were *hbg1* [5′-GCTTCTGACACAACTGTGTTCACTAGC-3'], used at a final concentration of 300 nM, and *hbg2* [5′-CACCAACTT CATCCACGTTCACC-3'], used at a final concentration of 700 nM. The final reaction mix contained 20 mM Tris-HCl, pH 8.4; 50 mM KCl; 200 mM each dNTP; 1% dimethyl sulfoxide; 0.4x Syber Green I; 22 ng *Escherichia coli* DNA per reaction; 0.4 Units of Platinum Taq DNA polymerase (Invitrogen Inc) per 11 mL reaction; ~6 ng of genomic DNA. Tubes containing 26, 8.75, 2.9, 0.97, 0.324, and 0.108 ng of a reference DNA (pooled human genomic DNA) were included in each PCR run so that the quantity of targeted templates in each research sample could be determined relative to the reference DNA sample by the standard curve method. The same reference DNA was used for all PCR runs. Baseline and follow-up samples from the same participant were assayed in the same batch.

To control for interassay variability, 8 control DNA samples were included in each run. In each batch, the T/S ratio of each control DNA was divided by the average T/S for the same DNA from 10 runs to get a normalizing factor. This was done for all 8 samples, and the average normalizing factor for all 8 samples was used to correct the participants' DNA samples and calculate the final T/S ratio. The T/S ratio for each sample was measured twice. When the duplicate T/S value and the initial value varied by more than 7%, the sample was run a third time, and the 2 closest values were reported. The average coefficient of variation for this study was 2.2%. The lab personnel who performed the assay were blind to all other outcomes.

2.3. Episodic memory

Verbal episodic memory was quantified using a 16-item list learning task, the California Verbal Learning Task, second edition

(CVLT-II; Delis et al., 2000). The primary outcome was the 20-minute free delayed-recall memory score, which has good short-term (ρ = 0.83) (Woods et al., 2006) and long-term (r = 0.69) (Alioto et al., 2017) test-retest reliability. CVLT-II delayed memory is sensitive to the deficits observed in the early stages of pathological aging and predicts progression from MCI to AD (Rabin et al., 2009). Visual episodic memory was quantified using the Benson Figure Test recall score. Participants drew a figure from memory that they had copied 10–15 minutes earlier (Kramer et al., 2003). Scores range from 0 to 17. The Benson Figure delayed recall score is sensitive to pathological aging (Kramer et al., 2003), and this measure is included in the Uniform Data Set battery. The Uniform Data Set is used by multicenter studies of aging and AD (https://www.alz.washington.edu/WEB/forms_uds.html).

2.4. Physical activity assessment

Physical activity was measured via the Physical Activity Scale for the Elderly (PASE), a brief self-administered questionnaire, which correlates with physiological measures of physical fitness (Washburn et al., 1999, 1993). The PASE evaluates physical activity over the past 7 days in 3 domains: recreational, household, and work-related. Participants rated their weekly frequency and daily duration for the following recreational activities: walking; light, moderate, and strenuous sports; and strength training. For each activity, a score was obtained by multiplying an activity frequency value by a task-specific weight provided by the scoring manual, such that, more strenuous activities are weighted more strongly (Washburn et al., 1993). A total score was calculated by summing the activity scores, with higher values indicating greater levels of current physical activity (Bolszak et al., 2014). To account for missing data, we calculated the average total PASE score across both visits, such that, if a participant only received this questionnaire at one time point, then this value would be taken as their PASE score at both time points. PASE scores were available at both time points in 31 participants, and at a single time point in 36 participants. Scores ranged from 10 to 291 (see Table 1).

2.5. Neuroimaging

2.5.1. Scanner information

Participants were scanned at the UCSF Neuroscience Imaging Center on a Siemens Trio 3T scanner. A T1-weighted magnetization prepared rapid gradient echo structural scan was acquired with an acquisition time of 8 minutes 53 seconds, sagittal orientation, field of view = 160 × 240 × 256 mm with an isotropic voxel resolution of 1 mm^3, repetition time = 2300 ms, echo time = 2.98 ms, inversion time = 900 ms, and flip angle = 9°. Diffusion-weighted images were acquired using single-short spin-echo sequence with the following parameters: repetition time = 5300 ms; echo time = 88 ms; inversion time = 2500 ms; flip angle = 90; field of view = 256*256 mm; 2 diffusion values of b = 0 and 1000 s/mm; 12 diffusion directions; 4 repeats; 40 slices; matrix size = 128*128; voxel size = 2 mm*2 mm; slice thickness = 3 mm; and generalized autocalibrating partial parallel acquisition = 2.

2.5.2. Longitudinal T1 processing

Before prepossessing, all T1-weighted images were visually inspected for quality control. Images with excessive motion or image artifact were excluded. T1-weighted images underwent bias field correction using the N3 algorithm, and the segmentation was performed using SPM12 (Wellcome Trust Center for Neuroimaging, London, UK, http://www.fil.ion.ucl.ac.uk/spm) unified segmentation (Ashburner and Friston, 2005). An intraparticipant template was created using the rigid body registration and nonlinear diffeomorphic warping proposed by the symmetric diffeomorphic registration for longitudinal MRI framework (Ashburner and Ridgway, 2012). The intraparticipant template was also segmented using SPM12's unified segmentation. A group template was generated from within-participant average gray and white matter tissues by rigid body registration and nonlinear warping using Diffeomorphic Anatomical Registration using Exponentiated Lie Algebra (Ashburner, 2007). Participants' native space gray and white matter were normalized, modulated, and smoothed in the group template using intraparticipant and interparticipant transformations. The applied smoothing used a Gaussian kernel with 4-mm full width half maximum. For statistical purposes, linear and nonlinear transformations between Diffeomorphic Anatomical Registration using Exponentiated Lie Algebra's space and International Consortium for Brain Mapping were applied (Mazziotta et al., 2001). Individual and averaged segmentations were carefully inspected to ensure no major segmentation or normalization errors. Quantification of the hippocampi at each time point was accomplished by transforming a standard parcellation atlas (Desikan et al., 2006) into International Consortium for Brain Mapping space and summing all modulated gray matter bilaterally within each parcellated region.

2.5.3. Diffusion imaging methods

Oxford Centre for Functional MRI of the Brain's Software Library (FSL) (Jenkinson et al., 2012) software was used to coregister the diffusion direction images with the b = 0 image, then a gradient direction eddy current and distortion correction were applied. Diffusion tensors were calculated using a nonlinear least-squares algorithm from Dipy (Garyfallidis et al., 2014). After quality control, participants' tensors (4 dimensional image) were registered linearly and nonlinearly into a common space using DTI ToolKit (Zhang et al., 2006). At baseline, participants' tensors were moved into a group template. DTI scalar maps of fractional anisotropy (FA) and mean diffusivity (MD) were calculated from the participants' tensors in the group template space. The bilateral fornix was extracted from the ICBM-DTI-81 white matter labels and tract atlas (Mori and Crain, 2005).

2.6. APOE *genotyping*

Genomic DNA was extracted from peripheral blood using standard protocols (Gentra PureGene Blood Kit, Qiagen, Inc, Valencia, CA, USA). Genotyping was performed using either TaqMan or Sequenom genotyping. TaqMan Allelic Discrimination Assay was used for *APOE* genotyping (rs429358 and rs7412) and was conducted on an ABI 7900HT Fast Real-Time PCR system (Applied Biosystems, Foster City, CA, USA) according to manufacturer's instructions.

The SpectroAquire and MassARRAY Typer Software packages (Sequenom, San Diego, CA, USA) were used for interpretation. Typer analyzer (v3.4.0.18) was used to review and analyze data. Twenty-four of 69 participants carried at least 1 $\varepsilon 4$ allele.

2.7. Statistical analysis

Cross-sectional relationships between baseline TL and variables of interest were assessed using linear regression. Age and gender were entered as covariates in all models. Total intracranial volume was entered in models that included brain volume, and education was entered in all models assessing the relationship between TL and cognition. TL was rescaled to improve interpretability, such that the unstandardized regression coefficients (b) correspond to 0.1-unit change in telomere T/S ratio. Mixed effects models with random intercepts were fitted to assess the longitudinal association of within-participant changes in TL with imaging and cognitive outcomes. Age, gender, and *APOE* genotype entered as covariates in

all longitudinal models; again, education and total intracranial volume were covaried when appropriate. First, rate of TL attrition was assessed using the interval between TL measurements as a continuous predictor, as well a baseline age * time interaction to determine whether age was a moderating factor in rate of TL decline. TL was then assessed as a longitudinal predictor. In these models, we decomposed TL into within- and between-person variance by entering baseline TL as a time-invariant predictor and change from baseline (TL−baseline TL) as a metric of within-person change. This transformation allowed us to assess within-person change independent of between-person variance, while also controlling for baseline TL, a strong predictor of telomeric attrition (Farzaneh-Far et al., 2010). For significant models, we added PASE total score to the model as a time-invariant covariate to conduct a post hoc assessment of whether physical activity level accounted for the observed relationships. We also conducted a post hoc analysis assessing the effect of vascular risk factors for any significant models. For each vascular risk factor, we created a binary variable indicating whether there was any history of hypertension, hyperlipidemia, heart attack, diabetes, or whether they were current smokers at the time of either visit. These values were summed for each person to create a vascular risk score that ranged from 0 to 5 (mean = 1, standard deviation = 0.73, range: 0–2) and entered this score as a predictor. All statistical analyses were performed in Stata 14.2; linear mixed effects models were fitted using the mixed command (StataCorp, 2015). The R ggplot2 package was used to create Fig. 1.

3. Results

3.1. Cross-sectional models

At baseline, when entered simultaneously, there was a trend for a negative relationship between age and TL ($b = -0.06$, 95%: confidence interval [CI] = −0.14, 0.01, $p = 0.097$), but TL did not differ by gender ($b = 0.38$, 95%: CI = −0.64, 1.40, $p = 0.457$). Baseline TL did not differ by *APOE ε4* status ($b = 0.08$, 95% CI = −1.01, 1.17, $p = 0.884$).

There was a trend for shorter TL to be associated with higher fornix MD ($b = -0.01$, 95% CI = −2.76, 0.07, $p = 0.062$). Baseline TL

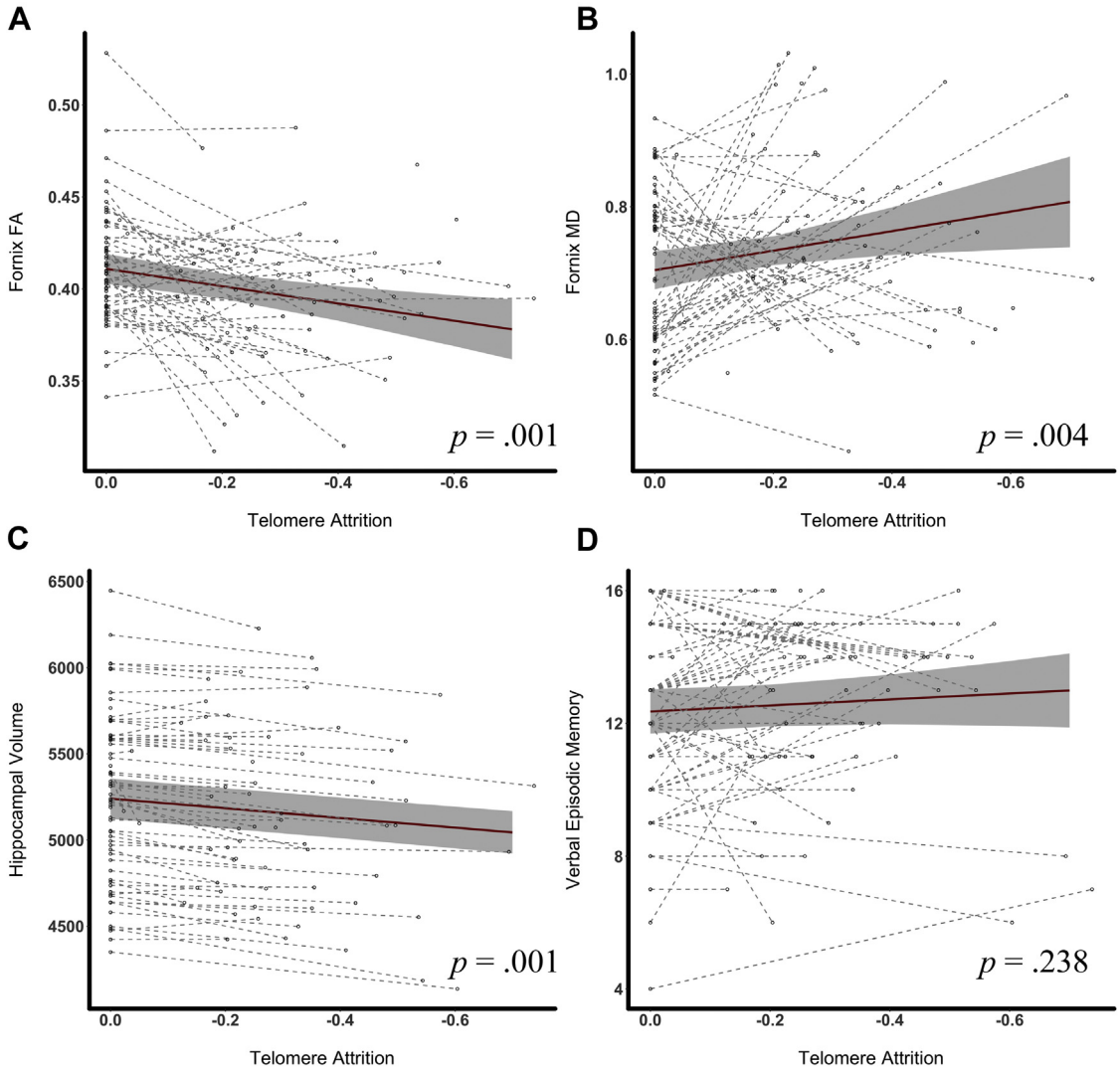

Fig. 1. Rate of telomere attrition is associated with the rate of hippocampal atrophy and decline in fornix microstructure in functionally normal older adults. Note: The dots in each figure represent individual data points. Dashed lines are used to connect data for each participant. The solid lines in each figure are fitted regression lines from linear mixed effects models with 95% confidence intervals. (A and B) plot TL against fornix FA and MD, respectively. (C) shows the relationship between telomere attrition and hippocampal volume (mm^3), and (D) illustrates the association between TL and California Verbal Learning Test, second edition (CVLT-II) long delay-free recall score (range: 0–16). Abbreviations: FA, fractional anisotropy; MD, mean diffusivity; TL, telomere length.

was not significantly associated with hippocampal volume ($b = -17.94$, 95% CI $= -67.37, 31.49$, $p = 0.471$), fornix FA ($b = 1.1 \times 10^{-3}$, 95% CI $= -0.003, 0.005$, $p = 0.567$), visual memory ($b = -0.12$, 95% CI $= -0.46, 0.22$, $p = 0.471$), or verbal memory ($b = -0.22$, 95% CI $= -0.55, 0.09$, $p = 0.158$) cross sectionally.

3.2. Longitudinal models

All participants showed declines in TL between baseline and follow-up, with an average annual TL attrition of 0.11 T/S units (standard deviation = 0.06). Older age at baseline was not associated with increased rates of telomere attrition ($b = 1.8 \times 10^{-4}$, 95% CI $= -0.02, 0.02$, $p = 0.861$). *APOE* genotype did not affect the rate of attrition ($b = -0.04$, 95% CI $= -0.31, 0.24$, $p = 0.804$). Neither verbal ($b = 0.14$, 95% CI $= -0.06, 0.33$, $p = 0.164$) nor visual memory ($b = 0.10$, 95% CI $= -0.21, 0.41$, $p = 0.548$) declined longitudinally, and in fact, demonstrated a slight (nonsignificant) improvement with time. With regard to neuroimaging variables, hippocampal volume decreased by an average of 30.35 mm^3/y (95% CI $= -39.02, -21.67$, $p < 0.001$), and global gray matter volume decreased by 3359.97 mm^3/y (95% CI $= -4341.86, -2378.09$, $p < 0.001$). Annual longitudinal changes were also observed for fornix FA ($b = -6.5 \times 10^{-3}$, 95% CI $= -9.59 \times 10^{-3}, -3.4 \times 10^{-3}$, $p < 0.001$) and fornix MD ($b = 0.02$, 95% CI $= 3.21 \times 10^{-3}, 0.03$, $p = 0.016$).

In contrast with the cross-sectional results, greater TL attrition was associated with faster rates of decline in hippocampal volume, with an estimated volume loss of 27.09 mm^3/y per 0.1-unit decline in T/S ratio (95% CI = 19.96, 34.21, $p < 0.001$). This relationship remained significant, albeit attenuated, even after controlling for global gray matter atrophy ($b = 10.83$, 95% CI = 4.05, 17.61, $p = 0.002$). This relationship also remained significant after controlling for physical activity level ($b = 26.43$, 95% CI = 19.12, 33.74, $p < 0.001$) or vascular risk score ($b = 27.8$, 95% CI = 20.97, 34.63, $p < 0.001$).

Greater TL attrition was also associated with faster rates of decline in fornix FA ($b = 4.4 \times 10^{-3}$, 95% CI = 0.002, 0.007, $p = 0.002$) and increases in fornix MD ($b = -0.01$, 95% CI $= -0.03, -0.003$, $p = 0.012$). The relationship with fornix FA ($b = 3.8 \times 10^{-3}$, 95% CI $= 1.07 \times 10^{-3}, 6.6 \times 10^{-3}$, $p = 0.007$) and MD ($b = -0.01$, 95% CI $= -0.02, -7.3 \times 10^{-4}$, $p = 0.037$) remained significant after controlling for physical activity. Similarly, these relationships remained after controlling for vascular risk: fornix FA ($b = 4.39 \times 10^{-3}$, 95% CI $= 1.69 \times 10^{-3}, 7.1 \times 10^{-3}$, $p = 0.001$) and MD ($b = -0.01$, 95% CI $= -0.03, -3.2 \times 10^{-3}$, $p = 0.012$).

Telomere attrition was not significantly correlated with verbal ($b = -0.1$, 95% CI = −0.26, 0.07, $p = 0.238$) or visual memory ($b = -0.17$, 95% CI = −0.41, 0.15, $p = 0.373$). Participant-specific trajectories are shown in Fig. 1 with a fitted regression line overlaid.

4. Discussion

In functionally intact older adults followed longitudinally, reductions in TL were associated with declining integrity of the fornix and hippocampal atrophy, even after controlling for global gray matter atrophy. Significant longitudinal relationships between telomere attrition and episodic memory were not observed. Memory scores did not decline over time, and in some cases increased, potentially indicating practice effects in this cognitively intact sample. Age and *APOE* genotype did not account for this relationship and were not associated with a faster rate of telomere attrition. In contrast with the longitudinal results, cross-sectional analyses did not reveal significant associations between TL and structure or function of the memory system. The present study also did not find a significant cross-sectional relationship between age and baseline TL, potentially because of our relatively small sample size. Alternatively, the lack of findings could be due to a survival bias in our older participants. In a study of 100,000 adults, a reversal in relationship between age and TL was seen in those over age 75 years, and other studies have also found longer TL in those who survive the longest (Nakamura et al., 2007; Rehkopf et al., 2013).

Our longitudinal findings are commensurate with the few cross-sectional studies that have explored the relationship between TL and brain structure and function in aging. In a cross-sectional, population-based study of 1960 individuals, TL was associated with total cerebral gray and white matter volume, particularly in parietal and temporal regions, including the hippocampi (King et al., 2014). Other cross-sectional work has shown TL correlates positively with hippocampal volume in healthy adults ages 49–66 years (Jacobs et al., 2014) as well as in a mixed sample of healthy and MCI women (Grodstein et al., 2008). Our work complements and extends these findings by showing the first longitudinal evidence of a relationship between the rate of telomere attrition and hippocampal volume loss in healthy older adults. Furthermore, this is the first study to show a relationship between TL and white matter microstructure as measured by DTI, a metric that is highly sensitive to aging and early neuropathological processes (Lockhart and DeCarli, 2014; Weiner et al., 2017). Our results suggest that the rate of telomere attrition may be a better biomarker of aging than cross-sectional quantification of TL. Similar findings have been described in several diseases of aging (Bekaert et al., 2005).

Telomere attrition reflects a combination of lifestyle, neuropathological, and genetic factors. Although human TL shortens across the lifespan, further attrition has been observed in states of disease that are common in aging and affect cognition and brain structure, such as oxidative stress (Tian et al., 2017), inflammation (Liu et al., 2010), and cardiovascular disease (Toupance et al., 2017). These disease states are also associated with neurodegenerative processes that affect the hippocampi and fornix (Oishi and Lyketsos, 2014; Weiner et al., 2017). In the present study, many participants had at least 1 vascular risk factor. We did not find evidence that the number of vascular risk factors modified the relationships between TL attrition and brain structure. Future studies using physiological measures of vascular risk will be important. Although our cohort is functionally normal, we know that neurodegenerative proteinopathies begin to accumulate years before symptom onset and are therefore likely present in the medial temporal lobes of some participants in this sample given their age range. In sporadic cases of AD, a recent meta-analysis found shorter TL in patients both at risk for (i.e., *APOE ε4* homozygotes) and with AD (Forero et al., 2016; Takata et al., 2012), and even in nondemented older adults, shorter TL may herald cognitive decline (Yaffe et al., 2011). Although telomeres were shorter in *ε4* carriers in the current sample, the relationship did not reach significance, despite its known role as a major AD risk gene (Genin et al., 2011). This lack of a relationship in our sample could be due to the small sample size and lack of statistical power.

The relationship we observed between TL and medial temporal lobe structures may also be mediated by other lifestyle factors. Because of the action of telomerase, telomeric DNA length is malleable in response to modifiable lifestyle factors. For instance, exercise and diet can slow telomere attrition (Ornish et al., 2013), and mindfulness meditation may increase TL (Conklin et al., 2018; Jacobs et al., 2011), whereas obesity (Chen et al., 2014), psychological stress (Epel et al., 2004), and cigarette smoking (Latifovic et al., 2016) are associated with telomere attrition. Many of these same factors impact neuroimaging metrics of brain structure (Duman, 2014; Kang et al., 2013; Morris et al., 2017). TL may therefore be associated with changes in brain structure because they both respond similarly to common neurobiological factors, both pathological and restorative. In this study, average physical

activity level did not affect the relationships we observed between TL attrition and brain structure. There are limitations to using the PASE as a proxy for exercise. First, we were missing too much data to include PASE level as a longitudinal covariate. Second, an objective, physiological measure of exercise capacity (e.g., VO_2 max) would reduce the biases associated with self-report measures. We did not gather information on diet at the time of this study, but future studies should examine the role of other lifestyle and health factors in mediating this relationship.

Thus far, we have discussed biological processes in aging that could simultaneously affect TL as well as brain structure. An alternative, or more likely complementary, hypothesis is that shortened TL engenders a cascade of events that alters brain structure. Emerging evidence indicates that telomere compromise promotes disease states in a positive feedback loop. Shortened TL can trigger cellular senescence, apoptosis, and metabolic failure (Blackburn et al., 2015; Sahin et al., 2011) and perpetuate a proinflammatory state (Ghosh et al., 2012; Wu et al., 2016), although not all studies have supported a direct relationship between telomere function and inflammation (Khan et al., 2015; Lustig et al., 2017). Telomere damage can incite cell death in cultured neurons (Cheng et al., 2007), reduce neuritogenesis in animal models (Ferrón et al., 2009), and lower brain volumes in telomerase RNA component knockout mice (Khan et al., 2015). Further support for the casual influence of telomere dysfunction on human health is lent by the study of the "human telomere syndromes." These syndromes include genetic variants of telomere structural proteins and telomerase, which result in accelerate aging phenotypes marked by common characteristics of aging such as graying, myocardial infarction, diabetes, and changes in skin pigmentation (Armanios and Blackburn, 2012). The relationship between TL, brain structure, and myriad neurobiological processes is likely highly complex and interactive, rather than unidirectional, and requires continued scientific inquiries.

There are several limitations to the present study. We measured TL in the periphery. It is unclear the degree to which these measurements are surrogates for central nervous system TL. The relationship between neural TL and leukocyte TL is variable across studies (Franco et al., 2006; Lukens et al., 2009; Thomas et al., 2008). This divergence may not be surprising, given that TL is largely a function of replication, and most neurons are postmitotic (Herrup et al., 2004). Worth noting, however, is that TL in several somatic tissues (not including neural cells) with differing replication rates are highly correlated, and this relationship is stable across adulthood (Daniali et al., 2013). In addition to being a function of replication, leukocyte TL may be directly associated with systemic or immune-mediated processes, such as oxidative stress, which also affect cells in the central nervous system. Telomeric DNA is especially vulnerable to reactive oxygen species, the DNA damage response and repair pathways are suppressed at telomeres, and telomerase activity may be inhibited by oxidative stress (Ahmed and Lingner, 2018). Another methodological limitation is that we averaged across leukocyte subtypes. There is substantial variability across subtypes (Lin et al., 2010), and therefore, part of the variation in TL between baseline and follow-up could reflect a shift in cell type rather than a reduction of length in the same proportion of cell types. For example, this has been proposed as potential contribution to the changing TL length observed in AD (Eitan et al., 2014). We did not measure telomerase levels, which could help clarify the relationship between telomeres and the aging brain. Finally, a greater number of follow-up visits would be needed to power a study assessing the directionality of the relationships observed in this study. For instance, it is plausible that declining brain structure (and the associated pathologic changes) begets telomeric attrition. Despite these limitations, our study is the first to demonstrate longitudinal relationships between TL, neuroimaging, and processing speed in older adults. Future work is needed to understand whether these results apply in patients with known AD pathology.

In conclusion, greater telomere attrition is associated with faster rates of hippocampal volume loss and larger declines in the white matter integrity of the fornix, above and beyond age in otherwise clinically normal older adults. This relationship may reflect neurobiological influences that affect both TL and brain structure, or the role of shortening TL rate on brain aging via pathways such as cellular senescence and inflammation. Longitudinal studies that quantify telomere attrition may continue to inform our understanding of the neurobiology of healthy aging and preclinical disease. Further work studying the potential of telomere attrition as a biomarker of early pathological aging is warranted.

Disclosure statement

Jue Lin is a cofounder and scientific advisor to Telomere Diagnostic Inc. The company played no role in this study.

Acknowledgements

This work was supported by the NIH-NIA [R01AG032289, R01AG048234, UCSF ADRC P50 AG023501] and the Larry L. Hillblom Network.

References

Ahmed, W., Lingner, J., 2018. Impact of oxidative stress on telomere biology. Differentiation 99, 21–27.
Albert, M.S., DeKosky, S.T., Dickson, D., Dubois, B., Feldman, H.H., Fox, N.C., Gamst, A., Holtzman, D.M., Jagust, W.J., Petersen, R.C., Snyder, P.J., Carrillo, M.C., Thies, B., Phelps, C.H., 2011. The diagnosis of mild cognitive impairment due to Alzheimer's disease: recommendations from the National Institute on Aging-Alzheimer's Association workgroups on diagnostic guidelines for Alzheimer's disease. Alzheimers Dement 7, 270–279.
Alioto, A.G., Kramer, J.H., Borish, S., Neuhaus, J., Saloner, R., Wynn, M., Foley, J.M., 2017. Long-term test-retest reliability of the California Verbal Learning Test - second edition. Clin. Neuropsychol. 31, 1449–1458.
Armanios, M., Blackburn, E.H., 2012. The telomere syndromes. Nat. Rev. Genet. 13, 693–704.
Ashburner, J., 2007. A fast diffeomorphic image registration algorithm. Neuroimage 38, 95–113.
Ashburner, J., Friston, K.J., 2005. Unified segmentation. Neuroimage 26, 839–851.
Ashburner, J., Ridgway, G.R., 2012. Symmetric diffeomorphic modeling of longitudinal structural MRI. Front. Neurosci. 6, 197.
Bekaert, S., De Meyer, T., Van Oostveldt, P., 2005. Telomere attrition as ageing biomarker. Anticancer. Res. 25, 3011–3021.
Blackburn, E.H., Epel, E.S., Lin, J., 2015. Human telomere biology: a contributory and interactive factor in aging, disease risks, and protection. Science 350, 1193–1198.
Blackburn, E.H., Greider, C.W., Szostak, J.W., 2006. Telomeres and telomerase: the path from maize, Tetrahymena and yeast to human cancer and aging. Nat. Med. 12, 1133–1138.
Bolszak, S., Casartelli, N.C., Impellizzeri, F.M., Maffiuletti, N.A., 2014. Validity and reproducibility of the Physical Activity Scale for the Elderly (PASE) questionnaire for the measurement of the physical activity level in patients after total knee arthroplasty. BMC. Musculoskelet. Disord. 15, 46.
Cawthon, R.M., 2002. Telomere measurement by quantitative PCR. Nucleic. Acids. Res. 30, e47.
Chen, S., Yeh, F., Lin, J., Matsuguchi, T., Blackburn, E., Lee, E.T., Howard, B.V., Zhao, J., 2014. Short leukocyte telomere length is associated with obesity in American Indians: the strong heart family study. Aging (Albany NY) 6, 380–389.
Cheng, A., Shin-ya, K., Wan, R., Tang, S., Miura, T., Tang, H., Khatri, R., Gleichman, M., Ouyang, X., Liu, D., Park, H.-R., Chiang, J.Y., Mattson, M.P., 2007. Telomere protection mechanisms change during neurogenesis and neuronal maturation: newly generated neurons are hypersensitive to telomere and DNA damage. J. Neurosci. 27, 3722–3733.
Conklin, Q.A., King, B.G., Zanesco, A.P., Lin, J., Hamidi, A.B., Pokorny, J.J., Álvarez-López, M.J., Cosín-Tomás, M., Huang, C., Kaliman, P., Epel, E.S., Saron, C.D., 2018. Insight meditation and telomere biology: the effects of intensive

retreat and the moderating role of personality. Brain. Behav. Immun. 70, 233–245.
Daniali, L., Benetos, A., Susser, E., Kark, J.D., Labat, C., Kimura, M., Desai, K., Granick, M., Aviv, A., 2013. Telomeres shorten at equivalent rates in somatic tissues of adults. Nat. Commun. 4, 1597.
Delis, D.C., Kramer, J.H., Kaplan, E., Ober, B.A., 2000. California verbal learning test - second edition. Adult version manual. Psychological Corporation, San Antonio, TX.
Desikan, R.S., Ségonne, F., Fischl, B., Quinn, B.T., Dickerson, B.C., Blacker, D., Buckner, R.L., Dale, A.M., Maguire, R.P., Hyman, B.T., Albert, M.S., Killiany, R.J., 2006. An automated labeling system for subdividing the human cerebral cortex on MRI scans into gyral based regions of interest. Neuroimage 31, 968–980.
Duman, R.S., 2014. Neurobiology of stress, depression, and rapid acting antidepressants: remodeling synaptic connections. Depress. Anxiety. 31, 291–296.
Dumurgier, J., Hanseeuw, B.J., Hatling, F.B., Judge, K.A., Schultz, A.P., Chhatwal, J.P., Blacker, D., Sperling, R.A., Johnson, K.A., Hyman, B.T., Gómez-Isla, T., 2017. Alzheimer's disease biomarkers and future decline in cognitive normal older adults. J. Alzheimers Dis. 60, 1451–1459.
Eitan, E., Hutchison, E.R., Mattson, M.P., 2014. Telomere shortening in neurological disorders: an abundance of unanswered questions. Trends. Neurosci. 37, 256–263.
Epel, E.S., Blackburn, E.H., Lin, J., Dhabhar, F.S., Adler, N.E., Morrow, J.D., Cawthon, R.M., 2004. Accelerated telomere shortening in response to life stress. Proc. Natl. Acad. Sci. U S A 101, 17312–17315.
Farzaneh-Far, R., Lin, J., Epel, E., Lapham, K., Blackburn, E., Whooley, M.A., 2010. Telomere length trajectory and its determinants in persons with coronary artery disease: longitudinal findings from the heart and soul study. PLoS One 5, e8612.
Ferrón, S.R., Marqués-Torrejón, M.A., Mira, H., Flores, I., Taylor, K., Blasco, M.A., Fariñas, I., 2009. Telomere shortening in neural stem cells disrupts neuronal differentiation and neuritogenesis. J. Neurosci. 29, 14394–14407.
Fletcher, E., Gavett, B., Harvey, D., Farias, S.T., Olichney, J., Beckett, L., DeCarli, C., Mungas, D., 2018. Brain volume change and cognitive trajectories in aging. Neuropsychology. https://doi.org/10.1037/neu0000447 [Epub ahead of print].
Fletcher, E., Raman, M., Huebner, P., Liu, A., Mungas, D., Carmichael, O., DeCarli, C., 2013. Loss of fornix white matter volume as a predictor of cognitive impairment in cognitively normal elderly individuals. JAMA Neurol. 70, 1389–1395.
Forero, D.A., González-Giraldo, Y., López-Quintero, C., Castro-Vega, L.J., Barreto, G.E., Perry, G., 2016. Meta-analysis of telomere length in Alzheimer's disease. J. Gerontol. A. Biol. Sci. Med. Sci. 71, 1069–1073.
Franco, S., Blasco, M.A., Siedlak, S.L., Harris, P.L.R., Moreira, P.I., Perry, G., Smith, M.A., 2006. Telomeres and telomerase in Alzheimer's disease: epiphenomena or a new focus for therapeutic strategy? Alzheimers Dement 2, 164–168.
Garyfallidis, E., Brett, M., Amirbekian, B., Rokem, A., van der Walt, S., Descoteaux, M., Nimmo-Smith, I. Dipy Contributors, 2014. Dipy, a library for the analysis of diffusion MRI data. Front. Neuroinform. 8, 8.
Genin, E., Hannequin, D., Wallon, D., Sleegers, K., Hiltunen, M., Combarros, O., Bullido, M.J., Engelborghs, S., De Deyn, P., Berr, C., Pasquier, F., Dubois, B., Tognoni, G., Fiévet, N., Brouwers, N., Bettens, K., Arosio, B., Coto, E., Del Zompo, M., Mateo, I., Epelbaum, J., Frank-Garcia, A., Helisalmi, S., Porcellini, E., Pilotto, A., Forti, P., Ferri, R., Scarpini, E., Siciliano, G., Solfrizzi, V., Sorbi, S., Spalletta, G., Valdivieso, F., Vepsäläinen, S., Alvarez, V., Bosco, P., Mancuso, M., Panza, F., Nacmias, B., Bossù, P., Hanon, O., Piccardi, P., Annoni, G., Seripa, D., Galimberti, D., Licastro, F., Soininen, H., Dartigues, J.-F., Kamboh, M.I., Van Broeckhoven, C., Lambert, J.C., Amouyel, P., Campion, D., 2011. APOE and Alzheimer disease: a major gene with semi-dominant inheritance. Mol. Psychiatry 16, 903–907.
Ghosh, A., Saginc, G., Leow, S.C., Khattar, E., Shin, E.M., Yan, T.D., Wong, M., Zhang, Z., Li, G., Sung, W.-K., Zhou, J., Chng, W.J., Li, S., Liu, E., Tergaonkar, V., 2012. Telomerase directly regulates NF-κB-dependent transcription. Nat. Cell Biol. 14, 1270–1281.
Grodstein, F., van Oijen, M., Irizarry, M.C., Rosas, H.D., Hyman, B.T., Growdon, J.H., De Vivo, I., 2008. Shorter telomeres may mark early risk of dementia: preliminary analysis of 62 participants from the nurses' health study. PLoS One 3, e1590.
Herrup, K., Neve, R., Ackerman, S.L., Copani, A., 2004. Divide and die: cell cycle events as triggers of nerve cell death. J. Neurosci. 24, 9232–9239.
Jacobs, E.G., Epel, E.S., Lin, J., Blackburn, E.H., Rasgon, N.L., 2014. Relationship between leukocyte telomere length, telomerase activity, and hippocampal volume in early aging. JAMA Neurol. 71, 921–923.
Jacobs, T.L., Epel, E.S., Lin, J., Blackburn, E.H., Wolkowitz, O.M., Bridwell, D.A., Zanesco, A.P., Aichele, S.R., Sahdra, B.K., MacLean, K.A., King, B.G., Shaver, P.R., Rosenberg, E.L., Ferrer, E., Wallace, B.A., Saron, C.D., 2011. Intensive meditation training, immune cell telomerase activity, and psychological mediators. Psychoneuroendocrinology 36, 664–681.
Jenkinson, M., Beckmann, C.F., Behrens, T.E.J., Woolrich, M.W., Smith, S.M., 2012. FSL. Neuroimage 62, 782–790.
Kang, D.-H., Jo, H.J., Jung, W.H., Kim, S.H., Jung, Y.-H., Choi, C.-H., Lee, U.S., An, S.C., Jang, J.H., Kwon, J.S., 2013. The effect of meditation on brain structure: cortical thickness mapping and diffusion tensor imaging. Soc. Cogn. Affect. Neurosci. 8, 27–33.
Khan, A.M., Babcock, A.A., Saeed, H., Myhre, C.L., Kassem, M., Finsen, B., 2015. Telomere dysfunction reduces microglial numbers without fully inducing an aging phenotype. Neurobiol. Aging 36, 2164–2175.
King, K.S., Kozlitina, J., Rosenberg, R.N., Peshock, R.M., McColl, R.W., Garcia, C.K., 2014. Effect of Leukocyte Telomere Length on Total and Regional Brain Volumes in a Large Population-Based Cohort. JAMA Neurol. 71, 1247–1254.
Kramer, J.H., Jurik, J., Sha, S.J., Rankin, K.P., Rosen, H.J., Johnson, J.K., Miller, B.L., 2003. Distinctive neuropsychological patterns in frontotemporal dementia, semantic dementia, and Alzheimer disease. Cogn. Behav. Neurol. 16, 211–218.
Latifovic, L., Peacock, S.D., Massey, T.E., King, W.D., 2016. The influence of Alcohol consumption, cigarette smoking, and physical activity on leukocyte telomere length. Cancer Epidemiol. Biomarkers Prev. 25, 374–380.
Lin, J., Epel, E., Cheon, J., Kroenke, C., Sinclair, E., Bigos, M., Wolkowitz, O., Mellon, S., Blackburn, E., 2010. Analyses and comparisons of telomerase activity and telomere length in human T and B cells: insights for epidemiology of telomere maintenance. J. Immunol. Methods 352, 71–80.
Liu, J.P., Chen, S.M., Cong, Y.S., Nicholls, C., Zhou, S.F., Tao, Z.Z., Li, H., 2010. Regulation of telomerase activity by apparently opposing elements. Ageing Res. Rev. 9, 245–256.
Lockhart, S.N., DeCarli, C., 2014. Structural imaging measures of brain aging. Neuropsychol. Rev. 24, 271–289.
Lukens, J.N., Van Deerlin, V., Clark, C.M., Xie, S.X., Johnson, F.B., 2009. Comparisons of telomere lengths in peripheral blood and cerebellum in Alzheimer's disease. Alzheimers Dement 5, 463–469.
Lustig, A., Liu, H.B., Metter, E.J., An, Y., Swaby, M.A., Elango, P., Ferrucci, L., Hodes, R.J., Weng, N., 2017. Telomere shortening, inflammatory cytokines, and anti-cytomegalovirus antibody follow distinct age-associated trajectories in humans. Front. Immunol. 8, 1027.
Mazziotta, J., Toga, A., Evans, A., Fox, P., Lancaster, J., Zilles, K., Woods, R., Paus, T., Simpson, G., Pike, B., Holmes, C., Collins, L., Thompson, P., MacDonald, D., Iacoboni, M., Schormann, T., Amunts, K., Palomero-Gallagher, N., Geyer, S., Parsons, L., Narr, K., Kabani, N., Le Goualher, G., Feidler, J., Smith, K., Boomsma, D., Pol, H.H., Cannon, T., Kawashima, R., Mazoyer, B., 2001. A four-dimensional probabilistic atlas of the human brain. J. Am. Med. Inform. Assoc. 8, 401–430.
McKhann, G.M., Knopman, D.S., Chertkow, H., Hyman, B.T., Jack Jr, C.R., Kawas, C.H., Klunk, W.E., Koroshetz, W.J., Manly, J.J., Mayeux, R., Mohs, R.C., Morris, J.C., Rossor, M.N., Scheltens, P., Carrillo, M.C., Thies, B., Weintraub, S., Phelps, C.H., 2011. The diagnosis of dementia due to Alzheimer's disease: recommendations from the National Institute on Aging-Alzheimer's Association workgroups on diagnostic guidelines for Alzheimer's disease. Alzheimers Dement 7, 263–269.
Mielke, M.M., Okonkwo, O.C., Oishi, K., Mori, S., Tighe, S., Miller, M.I., Ceritoglu, C., Brown, T., Albert, M., Lyketsos, C.G., 2012. Fornix integrity and hippocampal volume predict memory decline and progression to Alzheimer's disease. Alzheimers Dement 8, 105–113.
Mori, S., Crain, B.J., 2005. MRI Atlas of Human White Matter. Elsevier, Amsterdam.
Morris, J.K., Vidoni, E.D., Johnson, D.K., Van Sciver, A., Mahnken, J.D., Honea, R.A., Wilkins, H.M., Brooks, W.M., Billinger, S.A., Swerdlow, R.H., Burns, J.M., 2017. Aerobic exercise for Alzheimer's disease: a randomized controlled pilot trial. PLoS One 12, e0170547.
Nakamura, K.I., Takubo, K., Izumiyama-Shimomura, N., Sawabe, M., Arai, T., Kishimoto, H., Fujiwara, M., Kato, M., Oshimura, M., Ishii, A., Ishikawa, N., 2007. Telomeric DNA length in cerebral gray and white matter is associated with longevity in individuals aged 70 years or older. Exp. Gerontol. 42, 944–950.
Oishi, K., Lyketsos, C.G., 2014. Alzheimer's disease and the fornix. Front. Aging Neurosci. 6.
Ornish, D., Lin, J., Chan, J.M., Epel, E., Kemp, C., Weidner, G., Marlin, R., Frenda, S.J., Magbanua, M.J.M., Daubenmier, J., Estay, I., Hills, N.K., Chainani-Wu, N., Carroll, P.R., Blackburn, E.H., 2013. Effect of comprehensive lifestyle changes on telomerase activity and telomere length in men with biopsy-proven low-risk prostate cancer: 5-year follow-up of a descriptive pilot study. Lancet Oncol. 14, 1112–1120.
Rabin, L.A., Paré, N., Saykin, A.J., Brown, M.J., Wishart, H.A., Flashman, L.A., Santulli, R.B., 2009. Differential memory test sensitivity for diagnosing amnestic mild cognitive impairment and predicting conversion to Alzheimer's disease. Neuropsychol. Dev. Cogn. B Aging Neuropsychol. Cogn. 16, 357–376.
Rehkopf, D.H., Dow, W.H., Rosero-Bixby, L., Lin, J., Epel, E.S., Blackburn, E.H., 2013. Longer leukocyte telomere length in Costa Rica's Nicoya Peninsula: a population-based study. Exp. Gerontol. 48, 1266–1273.
Sahin, E., Colla, S., Liesa, M., Moslehi, J., Müller, F.L., Guo, M., Cooper, M., Kotton, D., Fabian, A.J., Walkey, C., Maser, R.S., Tonon, G., Foerster, F., Xiong, R., Wang, Y.A., Shukla, S.A., Jaskelioff, M., Martin, E.S., Heffernan, T.P., Protopopov, A., Ivanova, E., Mahoney, J.E., Kost-Alimova, M., Perry, S.R., Bronson, R., Liao, R., Mulligan, R., Shirihai, O.S., Chin, L., DePinho, R.A., 2011. Telomere dysfunction induces metabolic and mitochondrial compromise. Nature 470, 359–365.
Sfeir, A., de Lange, T., 2012. Removal of shelterin reveals the telomere end-protection problem. Science 336, 593–597.
StataCorp, 2015. Stata Statistical Software: Release 14. StataCorp LP, College Station, TX.
Takata, Y., Kikukawa, M., Hanyu, H., Koyama, S., Shimizu, S., Umahara, T., Sakurai, H., Iwamoto, T., Ohyashiki, K., Ohyashiki, J.H., 2012. Association between ApoE phenotypes and telomere erosion in Alzheimer's disease. J. Gerontol. A Biol. Sci. Med. Sci. 67, 330–335.
Thomas, P., O' Callaghan, N.J., Fenech, M., 2008. Telomere length in white blood cells, buccal cells and brain tissue and its variation with ageing and Alzheimer's disease. Mech. Ageing Dev. 129, 183–190.
Tian, R., Zhang, L.-N., Zhang, T.-T., Pang, H.-Y., Chen, L.-F., Shen, Z.-J., Liu, Z., Fang, Q., Zhang, S.-Y., 2017. Association between oxidative stress and peripheral leukocyte telomere length in patients with premature coronary artery disease. Med. Sci. Monit. 23, 4382–4390.
Toupance, S., Labat, C., Temmar, M., Rossignol, P., Kimura, M., Aviv, A., Benetos, A., 2017. Short telomeres, but not telomere attrition rates, are associated with carotid Atherosclerosis Novelty and significance. Hypertension 70, 420–425.
Washburn, R.A., McAuley, E., Katula, J., Mihalko, S.L., Boileau, R.A., 1999. The physical activity scale for the elderly (PASE): evidence for validity. J. Clin. Epidemiol. 52, 643–651.

Washburn, R.A., Smith, K.W., Jette, A.M., Janney, C.A., 1993. The physical activity scale for the elderly (PASE): development and evaluation. J. Clin. Epidemiol. 46, 153–162.
Weiner, M.W., Veitch, D.P., Aisen, P.S., Beckett, L.A., Cairns, N.J., Green, R.C., Harvey, D., Jack, C.R., Jagust, W., Morris, J.C., Petersen, R.C., Saykin, A.J., Shaw, L.M., Toga, A.W., Trojanowski, J.Q., 2017. Recent publications from the Alzheimer's Disease Neuroimaging Initiative: reviewing progress toward improved AD clinical trials. Alzheimers Dement 13, e1–e85.
Woods, S.P., Delis, D.C., Scott, J.C., Kramer, J.H., Holdnack, J.A., 2006. The California Verbal Learning Test - second edition: test-retest reliability, practice effects, and reliable change indices for the standard and alternate forms. Arch. Clin. Neuropsychol. 21, 413–420.
Wu, X., Yang, Y., Li, W., Cheng, Y., Li, X., Huang, C., Meng, X., Wu, B., Liu, X., Zhang, L., Lv, X., Li, J., 2016. Telomerase reverse transcriptase acts in a feedback loop with NF-κB pathway to regulate macrophage polarization in alcoholic liver disease. Sci. Rep. 6, 18685.
Yaffe, K., Lindquist, K., Kluse, M., Cawthon, R., Harris, T., Hsueh, W.C., Simonsick, E.M., Kuller, L., Li, R., Ayonayon, H.N., Rubin, S.M., Cummings, S.R., 2011. Telomere length and cognitive function in community-dwelling elders: findings from the Health ABC Study. Neurobiol. Aging 32, 2055–2060.
Zhang, H., Yushkevich, P.A., Alexander, D.C., Gee, J.C., 2006. Deformable registration of diffusion tensor MR images with explicit orientation optimization. Med. Image. Anal. 10, 764–785.